

The Thermodynamical Instability Induced by Pressure Ionization in Fluid Helium

Qiong Li¹, Hai-Feng Liu¹, Gong-Mu Zhang¹, Yan-Hong Zhao¹,
Guo Lu¹, Ming-Feng Tian¹, Hai-Feng Song¹
¹*Laboratory of Computational Physics,
Institute of Applied Physics and Computational Mathematics,
Beijing 100094, China*

A systematic study of pressure ionization is carried out in the chemical picture by the example of fluid helium. By comparing the variants of the chemical model, it is demonstrated that the behavior of pressure ionization depends on the construction of the free energy function. In the chemical model with the Coulomb free energy described by the Padé interpolation formula, thermodynamical instability induced by pressure ionization is found to be manifested by a discontinuous drop or a continuous fall and rise along the pressure-density curve as well as the pressure-temperature curve, which is very much like the first order liquid-liquid phase transition of fluid hydrogen from the first principles simulations. In contrast, in the variant chemical model with the Coulomb free energy term empirically weakened, no thermodynamical instability is induced when pressure ionization occurs, and the resulting equation of state achieves good agreement with the first principles simulations of fluid helium.

PACS numbers: 62.50.-p,52.25.Kn,64.70.Ja

I. INTRODUCTION

The thermodynamical properties of hydrogen/deuterium/helium have been intensively studied [1] over the past decades, due to its applications in astrophysics [2] and in inertial confinement fusion (ICF) research [3–5]. Over the wide range of densities and temperatures, the regime of partial dissociation/ionization has attracted particular attention, with the focus on the description of pressure dissociation/ionization, which is also of fundamental interest in condensed matter physics and remains a controversial problem. For helium, the studies [2, 6–9] in the framework of chemical models found a first order transition typically known as plasma phase transition; nonetheless, the first-principles simulations [10, 11] reached the opposite conclusion based on the calculated pressure-density relations which are perfectly smooth without any indication of first order transition.

In contrast, for hydrogen/deuterium, the first order transition connected with pressure ionization/dissociation was reported by both the chemical model [12] and the first-principles simulations [13–17]. For instance, Ref.[13] found a first order liquid-liquid transition for compressed hydrogen, which is signaled by large density fluctuations in a constant-pressure ensemble. By inspecting the pressure isochores, Refs.[16, 17] also reported signatures of a first order liquid-liquid transition, by showing a discontinuous drop in pressure on increasing temperature for deuterium [16], or by showing a smooth pressure isochore with a region of negative slope for hydrogen [17]. By inspecting the pressure isotherms for dense liquid hydrogen, Refs.[14, 15] further predicted the clear evidence of a first order liquid-liquid transition, which is a large drop in pressure on increasing density [14] or a smooth pressure isotherm with a plateau [15]. Note that these first-principles

simulations, although in agreement about the existence of the liquid-liquid phase transition, yield different results on the transition pressure and temperature [1]. Besides, there are also a few numerical studies such as Ref.[18], which do not report the first order liquid-liquid transition.

Obviously, whether pressure dissociation/ionization occurs smoothly or via a first order phase transition remains an open question. In partially ionized plasma of helium, there is no dissociation equilibrium interfering with the ionization equilibrium. Hence, helium is a better candidate than hydrogen for studying pressure ionization. In this paper, we are devoted to a close exploration of pressure ionization by the example of fluid helium, in the framework of chemical models similar to those used in Refs.[2, 9, 19, 20], and try to resolve the contradiction between the chemical models [2, 6–9] and the first principles simulations [10, 11] about the prediction of plasma phase transition in fluid helium, by examining the construction of the free energy function.

The rest of the paper is organized as follows. In Sec. II, the model is described. In Sec. III, the results and discussions are presented. Finally, the conclusions and outlooks are given.

II. THE MODEL

A. The chemical picture

The chemical picture assumes the existence of distinguishable chemical species - molecules, atoms, ions and electrons, which are interacting and reacting in equilibrium. For partially ionized plasma of helium, the chemical species include He, He⁺, He²⁺ and e, and the plasma composition is determined by ionization equilibrium equations, which are derived by minimizing the free

energy density with respect to the abundances of ionic species. The well-known Saha equation is established for non-interacting classical systems. Nevertheless, generally the interactions between plasma particles and the quantum nature of free electrons cannot be neglected. As a result, the general ionization equilibrium equations can be reformed as follows,

$$\frac{n_i}{n_{i-1}} = \frac{U_i}{U_{i-1}} \exp[-\xi - I_i^{\text{eff}}/k_B T], \quad (i = 1, \dots, Z_{\text{max}}) \quad (1)$$

which are also called generalized Saha equations. In comparison with Saha equation, the isolated ionization potential I_i is replaced by the effective ionization potential

$$I_i^{\text{eff}} = I_i - \left(\frac{\partial}{\partial N_{i-1}} - \frac{\partial}{\partial N_i} - \frac{\partial}{\partial N_e} \right) F^{\text{non-id}}, \quad (2)$$

which includes the chemical potential shift contributed by the interacting part of the free energy and is known as pressure-induced ionization potential lowering. Obviously, the plasma composition is determined by the effective ionization potentials, which are in turn determined by the interacting part of the free energy function. Therefore, the construction of the free energy function is of fundamental importance.

B. The free energy function

Then we shall present the chemical model used in this paper, by specifying the free energy function, which can be decomposed into the kinetic term, the ionization energy term including internal excitations, the Coulomb term, the configurational term, etc.

1. The kinetic free energy

The kinetic term, which is contributed by the translational motion of heavy particles (He , He^+ , He^{2+}) with Maxwell-Boltzmann statistics and that of free electrons with Fermi-Dirac statistics, can be written as

$$F_{\text{id}} = \sum_{i=0}^2 N_i k_B T \left[\ln \left(\frac{N_i}{V} \left(\frac{2\pi\hbar^2}{m_i k_B T} \right)^{3/2} \right) - 1 \right] + N_e k_B T \left(\xi - \frac{2}{3} \frac{I_{3/2}(\xi)}{I_{1/2}(\xi)} \right), \quad (3)$$

Here, N_0 , N_1 , N_2 and N_e are the numbers of He , He^+ , He^{2+} and e respectively, m_i is the mass of the corresponding heavy particle, $m_2 \simeq m_1 \simeq m_0 = m_{\text{He}}$, and the Fermi integrals are defined by

$$I_\nu(\xi) \equiv \int_0^\infty dx \frac{x^\nu}{e^{x-\xi} - 1}, \quad (\nu = 1/2, 3/2). \quad (4)$$

Note that the free part of the electronic chemical potential $\xi \equiv \mu_e^{\text{id}}/k_B T$ is determined by the number density of free electrons,

$$I_{1/2}(\xi) = \frac{\sqrt{\pi}}{4} \frac{N_e}{V} \left(\frac{2\pi\hbar^2}{m_e k_B T} \right)^{3/2}, \quad (5)$$

where the electronic spin has been taken into account.

2. The ionization free energy

The ionization energy term is given by

$$F_{\text{i-ex}} = -N_1 k_B T \ln 2 + N_1 I_1 + N_2 (I_1 + I_2), \quad (6)$$

where $I_1 = 24.6$ eV, $I_2 = 54.4$ eV. Note that the bound states of He and He^+ are included in the simplest way by ignoring all excited states, which is a good approximation when the temperature is much lower than the first excited level, since in this paper we are constrained to low temperatures when pressure effects dominate over temperature effects.

3. The Coulomb free energy

There remains no exact formula to calculate the Coulomb free energy of charged particles (free electrons, bare ions and ions with bound electrons). In the SCvH model [2], interactions between the charged particles, including He^{2+} , He^+ and e , are described by the Debye-Hückel approximation, which is constrained in the weak coupling regime. In Ref.[8], the Coulomb contributions are estimated in the framework of ion sphere model. In Refs.[9, 19, 20], the Padé interpolation formula, which have been developed for fully ionized plasma [21, 22], are used to describe the Coulomb interactions between charged particles in partially ionized plasma over a wide range of densities and temperatures. In this paper, we shall try the Padé interpolation formula for the approximate description of Coulomb interactions. The Coulomb term can be split into four parts as follows,

$$F_{\text{coul}} = F_{\text{ee}}^{\text{x}} + F_{\text{ee}}^{\text{c}} + F_{\text{ii}}^{\text{c}} + F_{\text{ie}}^{\text{c}}, \quad (7)$$

where x and c denote the exchange and the correlation terms respectively, F_{ee} and F_{ii} correspond to the electron and the ion fluid, F_{ie} describes the effect of the ion-electron interaction. The detailed formula of the four parts can be found in Ref.[21].

4. The configurational free energy

The He^+ ion, which carries a net charge and a bound electron, has both the charge nature and the finite size

nature, of which the former is considered in the Coulomb term, and the latter should be considered additionally. At low densities when the particles are far enough apart so that they feel only the Coulomb part of the He^+ potential but not the very short range effect of the bound electron, the finite size of He^+ can be neglected [2]. At high densities, the He^+ ions can be modeled by hard spheres with the diameter estimated as twice the expectation value of the radius r in the unperturbed hydrogen-like 1s-state, $d_1 = 1.5 a_B$, where a_B is the Bohr radius [7]. The diameter of the bare nuclei He^{2+} is neglected.

The interactions in the subsystem of neutral atoms are described by the hard-sphere variational formulation of fluid perturbation theory using the effective pair-wise additive potential, which takes the form of Aziz and Slaman [24] for $r \geq 1.8 \text{ \AA}$, and that of Ceperley and Partridge [25] for $r < 1.8 \text{ \AA}$. To mimic the softening due to many-body effects at high density, this effective pair potential is modified by a density-dependent function [8],

$$\tilde{\Phi}_{\text{eff}}(r) = \left(1 - C + \frac{C}{1 + D\rho}\right) \Phi_{\text{eff}}(r), \quad (8)$$

where the two parameters $(C, D) = (0.44, 0.8 \text{ cm}^3/\text{g})$ are optimized to reproduce the experimental measures of adiabatic sound velocity. Note that the fluid perturbation theory of the neutral subsystem is disturbed by the presence of the finite-sized He^+ ions. The mixture of the He^+ hard spheres and the hard core part of the He atoms is described by the Mansoori formula [26],

$$\begin{aligned} F_{\text{hc}}/Nk_B T &= -\frac{3}{2}(1 - y_1 + y_2 + y_3) + \frac{3y_2 + 2y_3}{1 - \eta} \\ &+ \frac{3}{2} \frac{1 - y_1 - y_2 - y_3/3}{(1 - \eta)^2} + (y_3 - 1) \ln(1 - \eta), \end{aligned} \quad (9)$$

where

$$\begin{aligned} y_1 &= \Delta_{01} \left(\sqrt{\frac{d_1}{d_0}} + \sqrt{\frac{d_0}{d_1}} \right), \\ y_2 &= \Delta_{01} \left(\frac{\eta_0}{\eta} \sqrt{\frac{d_1}{d_0}} + \frac{\eta_1}{\eta} \sqrt{\frac{d_0}{d_1}} \right), \\ y_3 &= \left[\left(\frac{\eta_0}{\eta} \right)^{2/3} x_0^{1/3} + \left(\frac{\eta_1}{\eta} \right)^{2/3} x_1^{1/3} \right]^3, \\ N &= N_0 + N_1 + N_2, \quad x_0 = N_0/N, \quad x_1 = N_1/N, \\ \eta &= \eta_0 + \eta_1, \quad \eta_0 = \frac{1}{6} \pi d_0^3 \frac{N_0}{V}, \quad \eta_1 = \frac{1}{6} \pi d_1^3 \frac{N_1}{V}, \\ \Delta_{01} &= \frac{\sqrt{\eta_0 \eta_1} (d_0 - d_1)^2}{\eta d_0 d_1} \sqrt{x_0 x_1}, \end{aligned} \quad (10)$$

with the He^+ hard sphere diameter $d_1 = 1.5 a_B$ and the He hard core diameter d_0 to be determined.

The perturbation part of the He-He interaction is given by

$$F_{\text{pert}} = \frac{2\pi N_0^2}{V} \int_{d_0}^{\infty} g_{\text{hs}}(r, \tilde{\eta}_0) \tilde{\Phi}_{\text{eff}}(r) r^2 dr, \quad (11)$$

where $g_{\text{hs}}(r, \tilde{\eta}_0)$ is the radial distribution function in a system of hard spheres with the packing fraction $\tilde{\eta}_0$. Note that the packing fraction $\tilde{\eta}_0$ means the ratio of the space occupied by the core part of the He atoms to the total space allowed for the He atoms. However, due to the presence of the He^+ ions, the total space allowed for the He atoms is decreased to be $V(1 - \eta_1)$, and consequently, the packing fraction can be estimated as $\tilde{\eta}_0 = \eta_0/(1 - \eta_1)$.

The He hard core diameter d_0 is determined by minimizing the configurational free energy $F_{\text{conf}} = F_{\text{hc}} + F_{\text{pert}}$.

5. The quantum correction of inter-atomic interaction

Note that when the de Broglie wavelength of He atoms becomes comparable to the range of the inter-atomic potential, the He atoms no longer interact as classical point-like particles, and consequently, the quantum effects should be included, which in the Wigner-Kirkwood expansion to the first non-vanishing term [2, 8, 20, 27] can be written as

$$F_{\text{qm}} = \frac{\hbar^2 N_0^2}{24 m_0 k_B T V} \int_{d_0}^{\infty} \nabla^2 \tilde{\Phi}_{\text{eff}}(r) g_{\text{hs}}(r, \tilde{\eta}_0) r^2 dr. \quad (12)$$

The strength of the quantum correction can be estimated by the parameter λ_{DB}/r_m , where λ_{DB} is the de Broglie wavelength of He atoms and r_m is the radial distance of the inter-atomic potential minimum.

C. The plasma composition and the thermodynamical quantities

By minimizing the total free energy function

$$F = F_{\text{id}} + F_{\text{i-ex}} + F_{\text{coul}} + F_{\text{conf}} + F_{\text{qm}}, \quad (13)$$

with respect to the abundances of the ionic species He^+ and He^{2+} , we obtain the free energy and the plasma composition simultaneously. Then the thermodynamical quantities such as pressure, internal energy, and entropy can be derived from the free energy by thermodynamic relations. Note that minimizing the free energy function to obtain the plasma composition is equivalent to solving the generalized Saha equations.

III. RESULTS AND DISCUSSIONS

The studies will proceed in two steps. First, we are to investigate the thermodynamical instability induced by

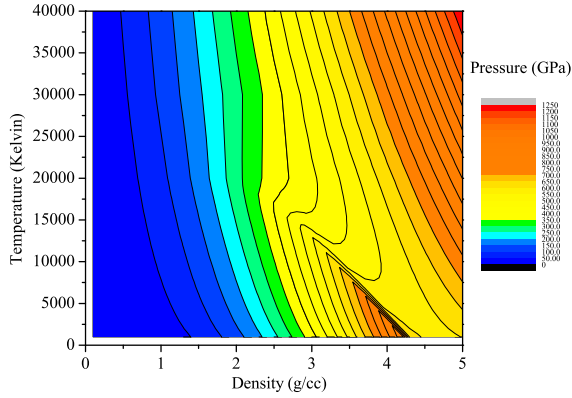


Figure 1: (Color online) The pressure contour plot of fluid helium as a function of temperature and density. A region of van der Waals-like loops can be observed.

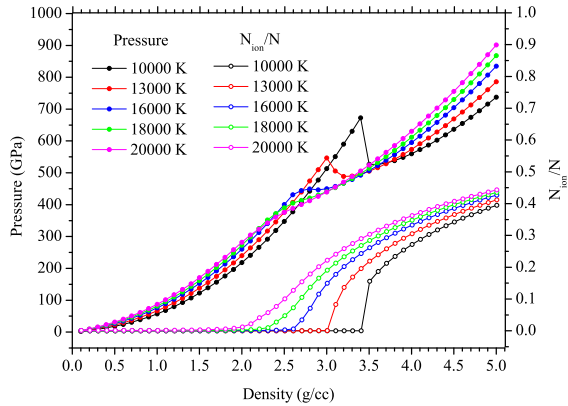


Figure 2: (Color online) The pressure and ionization degree of helium along various isotherms. The close connection between the behavior of the pressure curve and the density dependence of ionization degree is shown.

pressure ionization, based on the model described above. Then, we are to examine the construction of the free energy function and achieve good agreement with the first principles simulations [10, 11, 23] by weakening the Coulomb term.

A. The thermodynamical instability induced by pressure ionization

First we present the contour plot of the pressure calculated by the model described above, in a density region between 0.01 g/cc and 5.0 g/cc and for temperatures from 1000 K to 50000 K. As shown in Fig.1, a non-trivial region of van der Waals-like loops can be observed, which may be connected with pressure ionization. In order to study the details of van der Waals-like loops and how they are related to pressure ionization, we have plotted the pressure as well as the ionization degree along several se-

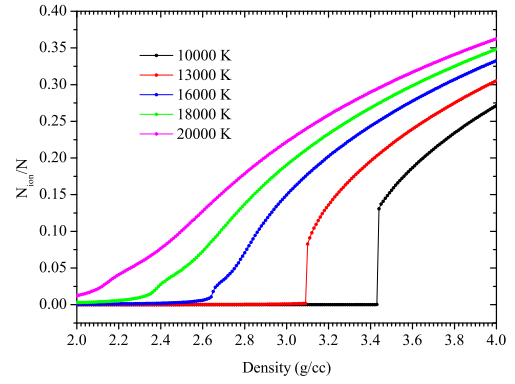


Figure 3: (Color online) The ionization degrees of helium along the isotherms are plotted at densely spaced density points. The curve of 10000 K is discontinuous between 3.43 g/cc and 3.44 g/cc. The curve of 13000 K is discontinuous between 3.09 g/cc and 3.10 g/cc. The curve of 16000 K is continuous, although it is extraordinarily steep between 2.64 g/cc and 2.66 g/cc.

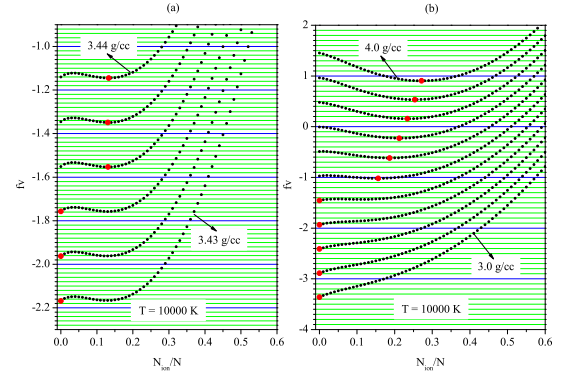


Figure 4: (Color online) The curves selected from the free energy surfaces over the ionic abundances. $N_1 = N_{\text{ion}}$, $N_2 = 0$, $f_v = F/Nk_B T$. Note that the plotted values of f_v include density-dependent shifts in order to make the curves more distinguishable. (a) The densities are equally spaced from 3.430 g/cc to 3.440 g/cc. (b) The densities are equally spaced from 3.0 g/cc to 4.0 g/cc. The red circle on each curve denotes its global minimum. The grid lines are shown to guide the eyes.

lected isotherms crossing the region of van der Waals-like loops. In order to study the temperature dependence of pressure ionization, we have plotted the pressure as well as the ionization degree along several selected isochores crossing the region of van der Waals-like loops.

It is important to highlight that the thermodynamical instability is generally located in the partial ionization regime of low temperatures and high densities when pressure effects dominate over temperature effects, because it is pressure ionization that causes the thermodynamical instability. Actually, by solving the Saha equations without the pressure-induced ionization potential lowering one can easily verify that the temperature ionization

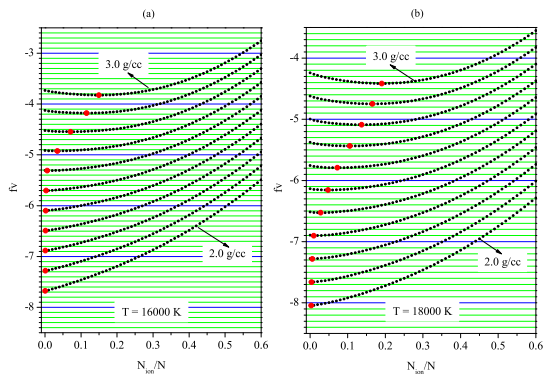


Figure 5: (Color online) The curves selected from the free energy surfaces over the ionic abundances. $N_1 = N_{\text{ion}}$, $N_2 = 0$, $f_v = F/Nk_B T$. Note that the plotted values of f_v include density-dependent shifts in order to make the curves more distinguishable. (a) $T=16000$ K. (b) $T = 18000$ K. The densities are equally spaced from 2.0 g/cc to 3.0 g/cc. The red circle on each curve denotes its global minimum. The grid lines are shown to guide the eyes.

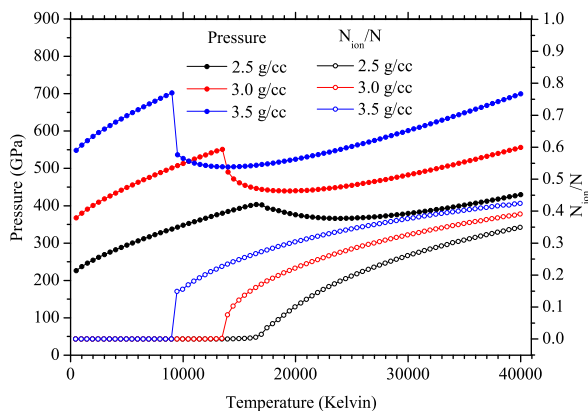


Figure 6: (Color online) The pressure and ionization degree of helium along various isochores at the densities of 2.5 g/cc, 3.0 g/cc and 3.5 g/cc. The close connection between the behavior of the pressure curve and the temperature dependence of ionization degree is shown.

always occurs smoothly and induces no thermodynamical instability.

1. The isotherms

The isotherms for selected temperatures crossing the region of van der Waals-like loops are plotted in Fig.2. It is seen that for 10000 K and 13000 K the pressure drops discontinuously at the top point of the van der Waals-like loop when the ionization degree jumps to a finite value abruptly, and for 16000 K the pressure remains smooth when ionization occurs continuously. As the temperature rises, the van der Waals-like loop becomes smaller and finally disappears. At higher temperatures of 18000

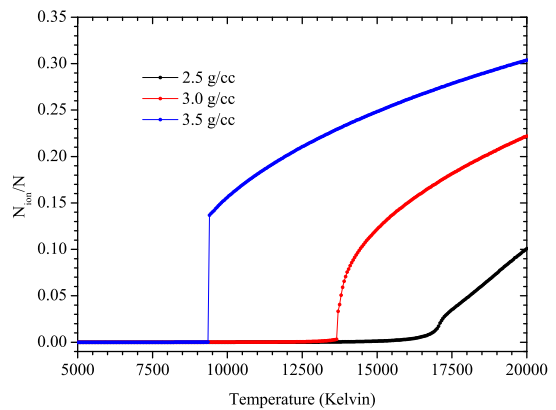


Figure 7: (Color online) The ionization degrees of helium along the isochores are plotted at densely spaced temperature points. The curve of 3.5 g/cc is drastically discontinuous between 9350 K and 9400 K. The curve of 3.0 g/cc is a bit discontinuous between 13300 K and 13350 K. The curve of 2.5 g/cc is continuous, although it is extraordinarily steep between 17000 K and 17250 K.

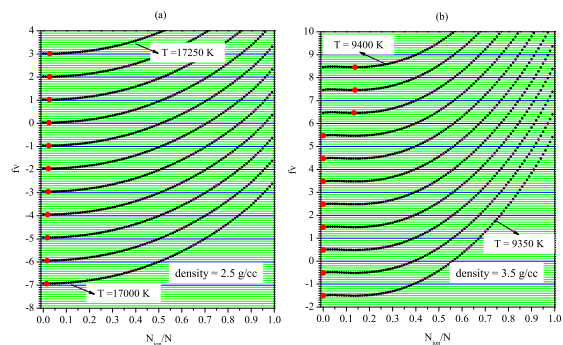


Figure 8: (Color online) The curves selected from the free energy surfaces over the ionic abundances. $N_1 = N_{\text{ion}}$, $N_2 = 0$, $f_v = F/Nk_B T$. Note that the values of f_v shown include temperature-dependent shifts in order to make the curves more distinguishable. (a) density = 2.5 g/cc. The temperatures are equally spaced from 17000 K to 17250 K. (b) density = 3.5 g/cc. The temperatures are equally spaced from 9350 K to 9400 K. The red circle on each curve denotes its global minimum. The grid lines are shown to guide the eyes.

K and 20000 K, the van der Waals-like loop has disappeared, but the slope of the pressure isotherm is still bent over, and as a result, the pressure of 18000 K is higher than that of 20000 K, which is opposite to the regions of both low densities and high densities. Note that the similar phenomenon of the coexistence pressure decreasing with the temperature was also found in hydrogen dissociation/ionization [12]. Above a critical temperature of about 20000 K, the thermodynamical instability disappears due to temperature effects.

In Fig.3 by plotting the ionization degrees at densely spaced density points, it is further confirmed that the

pressure ionization at sufficiently low temperatures occurs discontinuously and that at higher temperatures occurs continuously, which has yet to be explained. Note that the plasma composition is obtained by minimizing the free energy function with respect to the abundances of the ionic species He^+ and He^{2+} , so the straightforward way to explain the behavior of the ionization degree is by investigating the free energy surfaces over the abundances of ionic species, of which the minimum location corresponds to the plasma composition. We have examined the evolution of the free energy surface at the temperature of 10000 K with the increasing density, by inspecting it at equally spaced densities between the discontinuous points in Fig.3. Since throughout the evolution its minimum location is always on the line corresponding to $N_2/N = 0$, and hence, we only have to plot the free energy lines as a function of N_1/N . From Fig.4 it is found that the discontinuous rise of the ionization degree is due to the emergence of another local minimum which later becomes the global minimum abruptly. A similar examination is performed for the temperatures of 16000 K and 18000 K in Fig.5, which shows a single minimum shifting continuously.

From Figs.2 and 3 the behaviors of pressure ionization and its induced thermodynamical instability along the isotherms can be summarized as follows: along the isotherms of sufficiently low temperatures, the pressure ionization occurs discontinuously, which simultaneously induces a discontinuous drop of the pressure; along the isotherms of a little higher temperatures, the pressure ionization occurs continuously, which simultaneously induces a smooth van der Waals-like loop of the pressure; along the isotherms of even higher temperatures, the smooth van der Waals-like loop becomes smaller and finally disappears to become bending over; above the critical temperature, pressure ionization no longer causes thermodynamical instability, due to significant temperature effects. Note that the behaviors of the pressure-density relations here are in excellent agreement with those from the first principles simulations [14, 15].

2. The isochores

The isochores for selected densities crossing the region of van der Waals-like loops are plotted in Fig.6. Note that for high densities, there is a drop on the isochore, like the findings of the first principles simulations [16, 17] on hydrogen/deuterium. While the first principles simulations [16, 17] disagree whether the pressure isochore is a smooth curve with a region of negative slope or whether the pressure isochore has a discontinuous drop, the pressure isochores here demonstrate that both cases are possible. It is shown that at the density of 2.5 g/cc, the pressure isochore appears as a smooth curve with a negative slope region due to the continuous rise of the ionization degree, but at the higher densities of 3.0 g/cc and 3.5 g/cc, the pressure exhibits a discontinuous drop due

to the discontinuous rise of the ionization degree. The behavior of the ionization degree is further confirmed by the plot at densely spaced temperature points in Fig.7. The evolution of the free energy minimum with the rising temperature is shown in Fig.8. Since throughout the evolution the minimum of the free energy surface is always located on the line corresponding to $N_2/N = 0$, and hence, we only have to plot the free energy lines as a function of N_1/N . It is observed that at the density of 2.5 g/cc the single minimum shifts continuously with the rising temperature, while at the density of 3.5 g/cc another local minimum appears and gets lower with the rising temperature, so that at a certain temperature the global minimum shifts discontinuously from the local minimum of zero to that of a finite value.

From Figs.6 and 7 the behaviors of pressure ionization and its induced thermodynamical instability along the isochores can be summarized as follows: along the isochores of sufficiently high densities, the pressure ionization occurs discontinuously, which simultaneously induces a discontinuous drop of the pressure; along the isochores of a little lower densities, the pressure ionization occurs continuously, which simultaneously induces a continuous fall and rise of the pressure. Note that the behaviors of the pressure-temperature relations here are in excellent agreement with those from the first principles simulations [16, 17].

B. The examination of the free energy function

In the preceding subsection, we have shown the thermodynamical instability induced by pressure ionization based on the chemical model described in Sec.II. Nonetheless, the first principles simulations such as Refs. [10, 11] did not find any instability associated with pressure ionization in fluid helium. As is known, the plasma composition and the thermodynamic properties are determined by the free energy function, of which, therefore, a bit of uncertainty may bring changes to the pressure ionization phenomena. Note that the Coulomb free energy is described by the Padé interpolation formula [21] developed for fully ionized electron-ion plasma. Since there is currently no exact formula developed for describing the Coulomb energy among charged particles in partially ionized plasma, which is also beyond the scope of this paper, we have tried to tune the Coulomb term in a crude way and found that it achieves good agreement with the first principles simulations when the Coulomb term in Eq.(7) is weakened by a factor of $e^{-\Gamma_{\text{ion}}^{0.5}-\Gamma_e^{0.5}}$, with the Coulomb coupling parameters Γ_{ion} and Γ_e defined in Ref.[21].

1. No thermodynamical instability

Using the weakened Coulomb term, the studies on pressure ionization are repeated and the results are com-

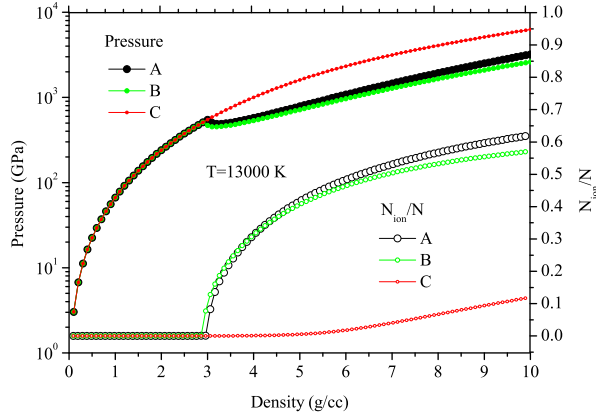


Figure 9: (Color online) The pressure and ionization degree of helium along the isotherm at the temperature of 13000 K, calculated by the chemical model and its variants. A: the original model. B: the model with $\tilde{\eta}_0 = \eta_0$. C: the model with the weakened Coulomb term.

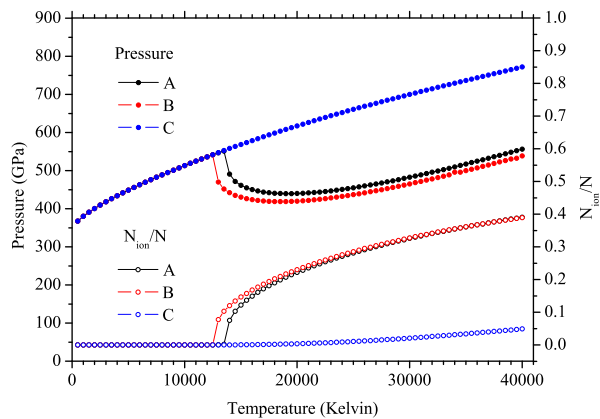


Figure 10: The pressure and ionization degree of helium along the isochore at the density of 3.0 g/cc, calculated by the chemical model and its variants. The meanings of “A, B, C” are the same as in Fig.9.

pared with the original model in Fig.9 and Fig.10. Note that the pressure ionization becomes strongly suppressed and brings no thermodynamical instability. In addition, the effect of the finite size of He^+ ions on the He fluid perturbation theory is also investigated, by repeating the calculations using the packing fraction of $\tilde{\eta}_0 = \eta_0$. It can be observed that the difference between the result of $\tilde{\eta}_0 = \eta_0$ and that of $\tilde{\eta}_0 = \eta_0/(1 - \eta_1)$ is relatively small and becomes more apparent with the increasing density.

2. The EOS in good agreement with the first principles simulations

The EOS models are usually checked by Hugoniot data. The double-shock Hugoniot curves are calculated by the original model, the model with $\tilde{\eta}_0 = \eta_0$ and the

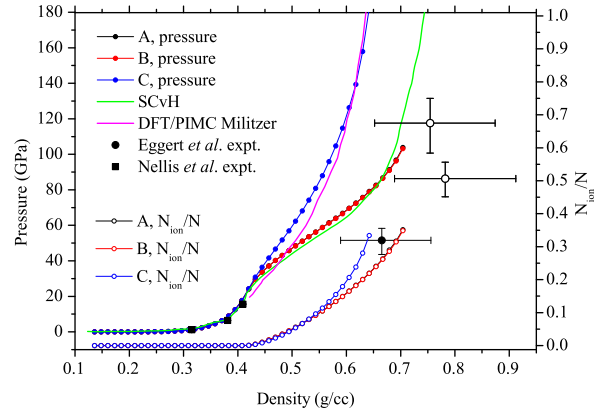


Figure 11: (Color online) The calculated Hugoniot data of fluid helium from (0.1235 g/cc, 4.3 K), including the pressure and the ionization degree. The meanings of “A, B, C” are the same as in Fig.9. Also shown are the first-shock data from Nellis *et al.* [28] (black square symbols), the shock data from Eggert *et al.* [29] (black circle symbols), the model calculation from SCvH [2] (green line) and the DFT/PIMC simulation from Ref.[23] (magenta line).

model with the weakened Coulomb term, using the initial states in accordance with the Nellis *et al.* experiment [28].

The first-shock curves are shown in Fig.11, in comparison with experimental data [28, 29] and other theoretical results [2, 23]. Note that the calculated Hugoniot curves begin to diverge when ionization occurs. The original model is in good agreement with the SCvH model [2], but much softer than the first principles simulation [23]. By using $\tilde{\eta}_0 = \eta_0$ the results are not much changed. By using the weakened Coulomb term, the calculated Hugoniot pressure is much enhanced to achieve good agreement with the first principles simulation [23]. As for the experimental data, the Nellis *et al.* shock data [28] has not reached the ionization regime, which thus cannot be employed to distinguish the chemical models; the Eggert *et al.* shock data [29] has indeed probed into the ionization regime, but its Hugoniot pressure is much lower than all the theoretical results. In Fig.12 the Hugoniot temperature is plotted versus the Hugoniot pressure. Note that the original model is in good agreement with the SCvH model [2], and the model with the weakened Coulomb term is slightly above the first principles simulation [23]. The experimental data [30] is relatively low, with the error bars covering some theoretical results.

The second-shock curves are shown in Fig.13, in comparison with experimental data [28] and first principles simulations [10, 23]. It is further confirmed that by using the weakened Coulomb term, the calculated Hugoniot pressure can be substantially enhanced and achieve good agreement with the first principles simulations [10, 23]. Note that the shock data of “QMD KHR” [10] is from a slightly different initial state.

The EOS models can also be checked by pressure isotherms. It can be observed from Fig.14 that the

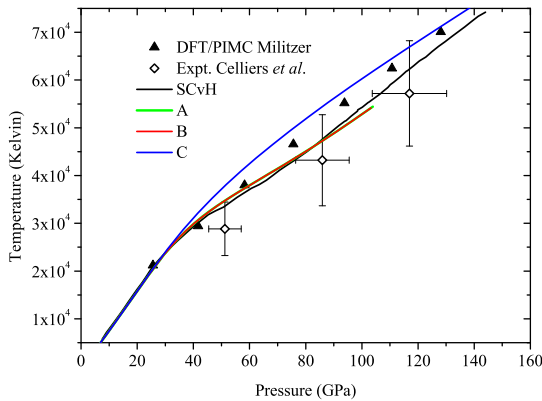


Figure 12: (Color online) The calculated Hugoniot temperature of fluid helium from (0.1235 g/cc, 4.3 K). The meanings of “A, B, C” are the same as in Fig.9. Also shown are the shock data from Celliers *et al.* [30] (open diamond symbols), the model calculation from SCvH [2] (black line) and the DFT/PIMC simulation from Ref.[23] (black triangles).

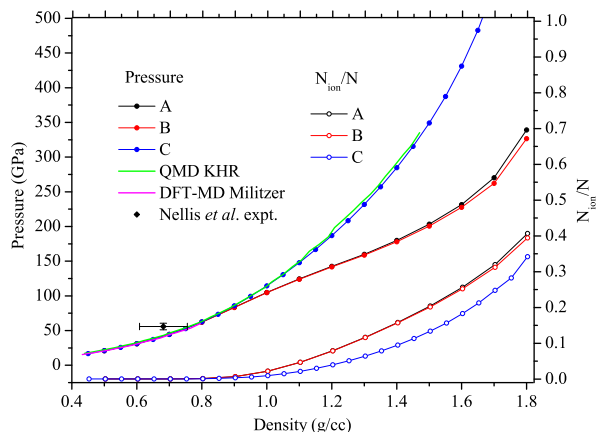


Figure 13: (Color online) The calculated Hugoniot data of fluid helium from (9.79 cc/mol, 13.8 GPa), including the pressure and the ionization degree. The meanings of “A, B, C” are the same as in Fig.9. Also shown are the second-shock data from Nellis *et al.* [28] (black diamond symbols) and the first principles simulation results of QMD KHR [10] and DFT-MD Militzer [23].

chemical models used in this paper are in much better agreement with the DFT/PIMC result [11] than the FKE chemical model [7]. The model with the weakened Coulomb term achieves particularly good agreement with the DFT/PIMC result [11]. As shown in Fig.15, the contour plot of the pressure from the model with the weakened Coulomb term does not exhibit any instability region, in contrast to the original model shown in Fig.1.

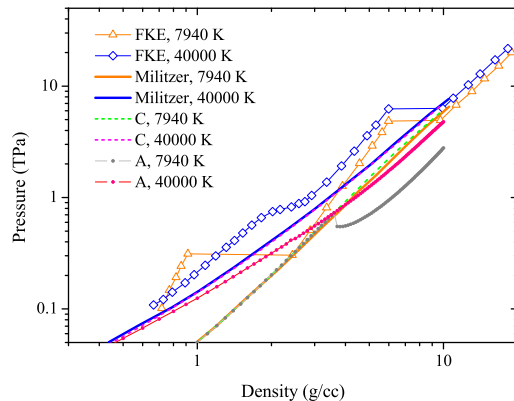


Figure 14: (Color online) The pressure isotherms calculated by the original model (A) and the model with the weakened Coulomb term (C) are shown, in comparison with the FKE chemical model (FKE) [7] and the first principles simulations (Militzer) [11].

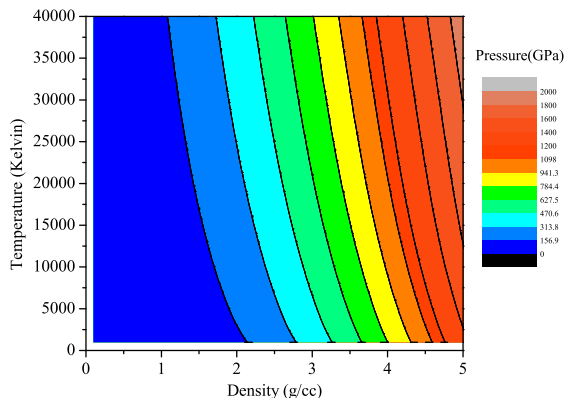


Figure 15: (Color online) The pressure contour plot of fluid helium, calculated from the model with the weakened Coulomb term.

IV. CONCLUSIONS AND OUTLOOKS

The pressure ionization has received intensive attention, due to fundamental interest in condensed matter physics, and also due to the importance in providing EOS for astrophysics and ICF research. In the first principles simulations, the pressure ionization of fluid hydrogen occurs via a first order liquid-liquid phase transition, and that of fluid helium, in contrast, occurs smoothly without any indication of first order transition. However, in the chemical model calculations the pressure ionization of fluid helium also occurs via a first order transition typically known as plasma phase transition. In this paper we have carried out a systematic study of pressure ionization in fluid helium, in the framework of chemical models. It is demonstrated that when pressure ionization occurs and whether it induces thermodynamical

stability are dependent on the construction of the free energy function. In the chemical model described in Sec. II, we have found the thermodynamical instability, which is induced by pressure ionization and is manifested by a discontinuous drop or a continuous fall and rise along the pressure-density and pressure-temperature curves. When the chemical model is modified by weakening the Coulomb term of the free energy function using an empirical factor, the pressure ionization occurs at higher densities and no longer induces thermodynamical instability. Moreover, the resulting smooth EOS achieves good agreement with the first principles simulations [10, 11, 23]. It is interesting that the thermodynamical instability induced by pressure ionization in fluid helium from the chemical model here is very much like that of the first order liquid-liquid phase transition of fluid hydrogen from the first principles simulations [14–17]. This implies that there may be some feature shared by the first principles simulations of molecular dissociation and the chemical model calculations of pressure ionization, which causes thermodynamical instability in the similar way. We guess that in analogy to the emergence

of another local minimum in the free energy surface in the chemical models, the first principles simulations may encounter another solution of the electronic Kohn-Sham equation.

Note that the great discrepancy between the first principles simulation results and the shock compression data in the regime of partial ionization remains to be resolved. Also note that the good agreement with the first principles simulation results is achieved by weakening the Coulomb term in a crude way, and it remains desirable to construct an accurate free energy function, especially the Coulomb term.

Acknowledgments

We are grateful to Qi-Li Zhang and Guang-Cai Zhang for helpful discussions. This work was supported by the National Science Foundation of China under Grants No.10804011 and No.11204015.

-
- [1] J. M. McMahon, M. A. Morales, C. Pierleoni, and D. M. Ceperley, *Rev. Mod. Phys.* **84**, 1607 (2012). and references therein.
 - [2] D. Saumon, G. Chabrier and H. M. Van Horn, *Astrophys. J. Suppl. Ser.* **99**, 713 (1995).
 - [3] S. X. Hu, B. Militzer, V. N. Goncharov, and S. Skupsky, *Phys. Rev. Lett.* **104**, 235003 (2010); *Phys. Rev. B* **84**, 224109 (2011).
 - [4] M. A. Morales *et al.*, *High Energy Density Phys.* **8**, 5 (2012).
 - [5] Cong Wang and Ping Zhang, *Phys. Plasmas* **20**, 092703 (2013).
 - [6] W. Ebeling, *Contrib. Plasma Phys.* **30**, 553 (1990).
 - [7] A. Förster, T. Kanhlbaum, and W. Ebeling, *Laser Part. Beams* **10**, 253 (1992).
 - [8] C. Winsidoerffer and G. Chabrier, *Phys. Rev. E* **71**, 026402 (2005).
 - [9] H. Juranek, V. Schwarz and R. Redmer, *J. Phys. A: Math. Gen.* **36**, 6181 (2003).
 - [10] A. Kietzmann, B. Holst, and R. Redmer, M. P. Desjarlais and T. R. Mattsson, *Phys. Rev. Lett.* **98**, 190602 (2007).
 - [11] B. Militzer, *Phys. Rev. B* **79**, 155105 (2009).
 - [12] D. Beule, W. Ebeling, A. Förster, H. Juranek, S. Nagel, R. Redmer, and G. Röpke, *Phys. Rev. B* **59**, 14177 (1999).
 - [13] S. Scandolo, *Proc. Natl. Acad. Sci. U.S.A.* **100**, 3051 (2003).
 - [14] W. Lorenzen, B. Holst, and R. Redmer, *Phys. Rev. B* **82**, 195107 (2010).
 - [15] M. A. Morales, C. Pierleoni, E. Schwegler, and D. M. Ceperley, *Proc. Natl. Acad. Sci. U.S.A.* **107**, 12799 (2010).
 - [16] S. A. Bonev, B. Militzer, and G. Galli, *Phys. Rev. B* **69**, 014101 (2004).
 - [17] J. Vorberger, I. Tamblyn, B. Militzer, and S. A. Bonev, *Phys. Rev. B* **75**, 024206 (2007).
 - [18] K. T. Delaney, C. Pierleoni, and D. M. Ceperley, *Phys. Rev. Lett.* **97**, 235702 (2006).
 - [19] V. Schwarz, H. Juranek and R. Redmer, *Phys. Chem. Chem. Phys.* **7**, 1990 (2005).
 - [20] Qifeng Chen, Ying Zhang, Lingcang Cai, Yunjun Gu, and Fuqian Jing, *Phys. Plasmas* **14**, 012703 (2007).
 - [21] W. Stolzmann and T. Blocker, *Astron. Astrophys.* **314**, 1024 (1996); **361**, 1152 (2000).
 - [22] G. Chabrier and A. Y. Potekhin, *Phys. Rev. E* **58**, 4941 (1998).
 - [23] B. Militzer, *Phys. Rev. Lett.* **97**, 175501 (2006).
 - [24] R. Aziz and M. Slaman, *J. Chem. Phys.* **94**, 8047 (1991).
 - [25] D. Ceperley and H. Partridge, *J. Chem. Phys.* **84**, 820 (1986).
 - [26] G. A. Mansoori, N. F. Carnahan, K. E. Starling, and T. W. Leland Jr., *J. Chem. Phys.* **54**, 1523 (1971).
 - [27] J. M. Aparicio and G. Chabrier, *Phys. Rev. E* **50**, 4948 (1994).
 - [28] W. J. Nellis, N. C. Holmes, A. C. Mitchell, R. J. Trainor, G. K. Governo, M. Ross, and D. A. Young, *Phys. Rev. Lett.* **53**, 1248 (1984).
 - [29] J. Eggert, S. Brygoo, P. Loubeyre, R. S. McWilliams, P. M. Celliers, D. G. Hicks, T. R. Boehly, R. Jeanloz, and G. W. Collins, *Phys. Rev. Lett.* **100**, 124503 (2008).
 - [30] P. M. Celliers *et al.*, *Phys. Rev. Lett.* **104**, 184503 (2010).